Mechanism of the visible electroluminescence from metal/porous silicon/n-Si devices

Tsuyoshi Oguro, Hideki Koyama, Tsuyoshi Ozaki, and Nobuyoshi Koshida

Citation: J. Appl. Phys. **81**, 1407 (1997); doi: 10.1063/1.363878
View online: http://dx.doi.org/10.1063/1.363878
View Table of Contents: http://jap.aip.org/resource/1/JAPIAU/v81/i3
Published by the American Institute of Physics.

Mechanism of the visible electroluminescence from metal/porous silicon/*n*-Si devices

Tsuyoshi Oguro,[a] Hideki Koyama,[b] Tsuyoshi Ozaki,[c] and Nobuyoshi Koshida
Division of Electronic and Information Engineering, Faculty of Technology, Tokyo University of Agriculture and Technology, Koganei, Tokyo 184, Japan

(Received 30 September 1996; accepted for publication 29 October 1996)

The excitation and radiative recombination mechanisms of carriers in electroluminescent porous silicon (PS) have been studied for the device with the structure of Au/PS/*n*-type Si. Experiments focus on the electroluminescence (EL) and photoluminescence (PL) spectra, the current-voltage-EL intensity relationship and its temperature dependence, and the excitation-wavelength dependence of the electric-field-induced PL quenching. The results of these experiments suggest the following points: (1) the EL occurs mainly near the Au/PS contact; (2) there exists an extremely high electric field at the Au/PS contact; (3) the EL originates from radiative recombination of strongly localized excitons; and (4) the radiative recombination rate is in proportion to the diode current. Based on these observations, an operation model is proposed. In our model, a large number of electrons and holes are generated in the PS layer by a field-assisted mechanism. Light emission occurs by radiative recombination of these electrons and holes via localized states. Because of field-enhanced carrier separation, however, the EL efficiency of this device is limited to a relatively low value of about 0.05%. Possible ways to improve the EL characteristics are discussed. © *1997 American Institute of Physics.* [S0021-8979(97)08303-5]

I. INTRODUCTION

Porous silicon (PS) has attracted much interest due to the property that it luminesces efficiently in the visible range even at room temperature.[1–4] Besides photoluminescence (PL),[5–7] visible electroluminescence (EL) has been obtained as well with either liquid[8,9] or solid-state[10–12] contact. While liquid-contact devices exhibit EL with high external quantum efficiencies comparable to that of PL, the EL efficiency of practically important solid-state-contact devices was fairly low at the early stage. The efficiency has been improved up to about 0.01%–0.2% by using PS layers made by anodizing *pn* junctions.[13–15] However, these values are still insufficient for practical uses. In addition, there remain some problems in stability and operation voltage. Another attempt is to form an impregnated contact with metals[16] or conducting polymers,[17,18] which aims at fabricating the same electrode configurations as in the case of efficient liquid-contact devices. The observed improvements by these device structures, however, are moderate and their efficiencies do not exceed the above mentioned value at present.

Understanding of the operation mechanism is very important in order to get a substantial improvement in the EL characteristics. Carrier injection into the porous layer has been assumed to be the case in many papers to explain the EL.[10,12,13,15,19] However, we should note that similar EL can be observed also in the metal/PS/*n*-Si structure[11,20,21] which does not contain any holes-supplying components. Investigation of the EL properties of this structure, therefore, will open another way to clarify the EL mechanism of PS-based devices.

In this article, we report fundamental characteristics of a metal/PS/*n*-Si diode in terms of the relation between the EL intensity and the operating variables (bias voltage, current, and temperature), as well as the relation between the EL and PL spectra. An experimental result is also presented on the excitation-wavelength dependence of the electric-field-induced PL quenching,[20,21] which gives us important information about the depth profile of the field intensity in the porous layer. Based on these experimental data, we propose a model that explains the performance of the device well. Key issues to improve the EL efficiency are discussed, which can also be applied to other structures of PS-based EL devices.

II. EXPERIMENT

Single-crystalline, (111)-oriented, and Sb-doped ($\sim$0.018 Ω cm in resistivity) Si wafers with an Al back contact were used as substrates. Anodization was carried out in a solution of 55% HF:ethanol=1:1 at 100 mA/cm^2 for 5 min. During the anodization, samples were illuminated by a 500 W tungsten lamp located at a distance of 20 cm. The thickness of the porous layer was $\sim$40 μm. Having been rinsed with ethanol for 2 min and dried, the samples were transferred into a vacuum chamber in which a thin, semitransparent Au film was deposited onto the PL layers.

Room temperature PL and EL measurements were conducted in a N_2 atmosphere in order to minimize oxidation effects. Keithley source-measure unit (Model 238) was employed as a voltage source and also as an ammeter of the diode current. The emitted light was dispersed and detected with a 25 cm monochromator (Nikon G250) and a photomul-

[a]Present address: Microcomputer Division, NEC Corp., Nakahara-ku, Kawasaki 211, Japan.
[b]Author to whom correspondence should be addressed. Electronic mail: koyama@cc.tuat.ac.jp
[c]Present address: Communication Technology Lab., Casio Computer Co., Ltd., Hamura-shi, Tokyo 205, Japan.

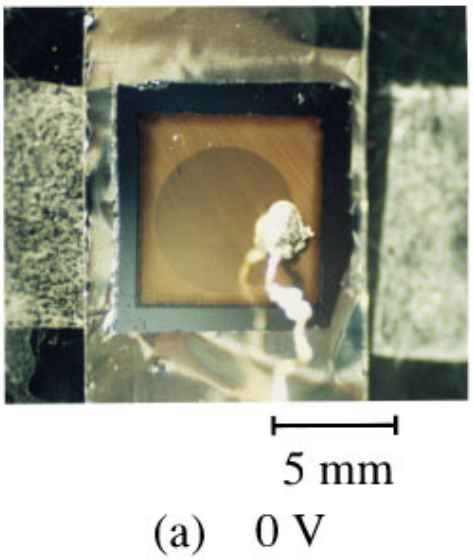

FIG. 1. Photographs of the EL device without (a) and with (b) a bias voltage of 50 V. Uniform light emission is observed under the bias voltage throughout the semitransparent Au contact. The emission is bright enough to be detected even in daylight.

tiplier tube (Hamamatsu R928), respectively. The spectral resolution in this experiment was <5 nm. A picoammeter (Advantest TR8652) was used to measure the output current of the photomultiplier tube. All this equipment was connected to a personal computer, which enables simultaneous control of the voltage source and monochromator as well as the measurements of current and EL intensity. All the measured PL and EL spectra were corrected for apparatus response. Low-temperature measurements were performed in vacuum using a Daikin UV202CL cryostat.

III. RESULTS

A. Fundamental EL characteristics at room temperature

Figures 1(a) and 1(b) show the photographs of our device without and with a bias voltage, respectively. Under sufficient bias voltages, uniform EL is clearly observed through the Au electrode even in daylight. Rough estimation of the external quantum efficiency yields a value of 0.05%.

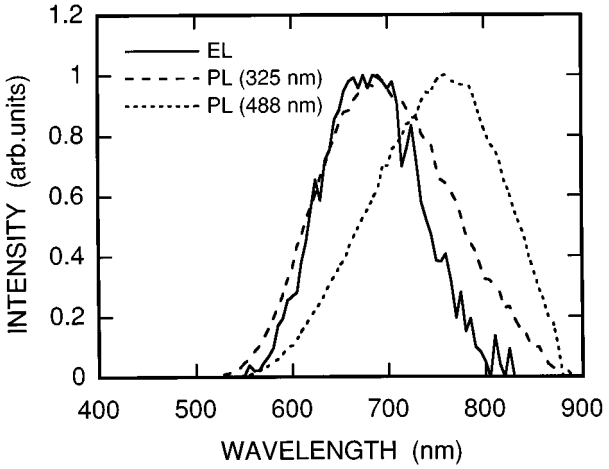

FIG. 2. EL and PL spectra of the same PS sample. The PL spectra are measured with two different-wavelength excitation beams (325 and 488 nm).

The EL spectrum of this device is shown in Fig. 2 by the solid curve. In this figure, the PL spectra of the active PS layer photoexcited at two different wavelengths are also shown by the dashed curves. It should be noted that the EL spectrum is close to the PL spectrum obtained from the shorter-wavelength excitation.

Figure 3 shows the current density and EL intensity at room temperature as a function of applied bias voltage. The inset shows the schematic diagram of the diode structure. The polarity of the voltage bias is defined such that it is positive when the front Au contact is positive with respect to the back Al contact. Hereafter we refer to the device as ''forward biased'' if the voltage is positive and ''reverse biased'' if the voltage is negative, as in the case of usual metal-semiconductor Schottky diodes. In fact, comparatively larger current flows under forward bias (positive voltages), as shown in Fig. 3. However, significant current flows also un-

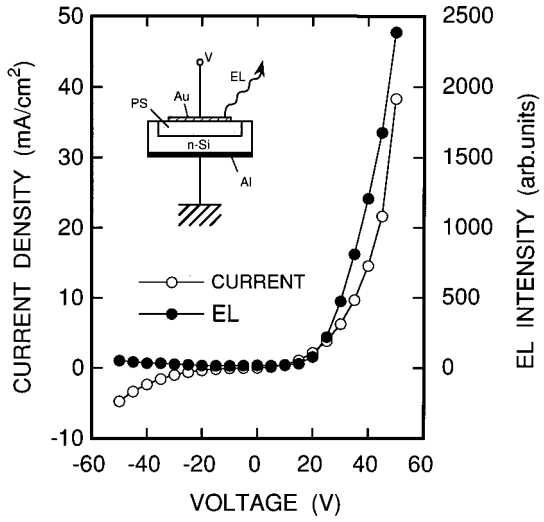

FIG. 3. Current density (open plots) and EL intensity (closed plots) at room temperature as a function of the bias voltage. Also shown in the inset is a schematic illustration of the device structure.

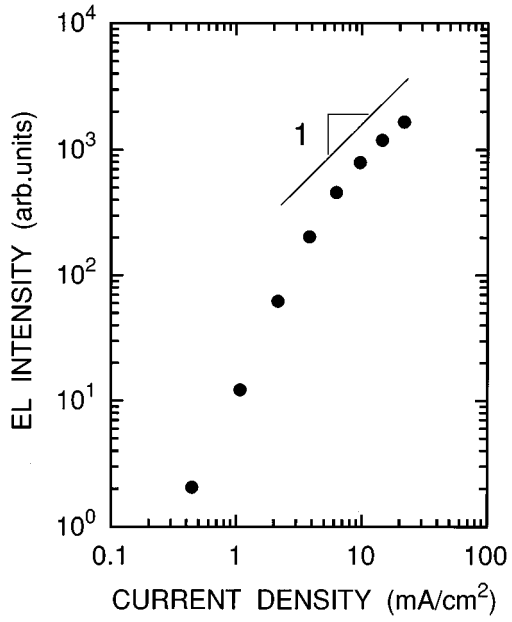

FIG. 4. EL intensity plotted as a function of current density. The straight line shows the slope of linear functions.

der reverse bias conditions. Correspondingly, EL is observed in both bias directions. We could not find any significant differences in EL spectra between forward and reverse bias. This polarity-independent property in EL spectrum has already been reported.[22] Another feature is that a large amount of current begins to flow at a relatively high voltage (~10 V) even in forward bias. This means that the diode ideality factor is quite large (in the present case more than one hundred) as described in previous reports.[10,12,23,24]

The EL intensity is plotted as a function of current density in Fig. 4. At sufficiently large current densities, the EL intensity increases in proportion to current as in usual light-emitting diodes. At low bias levels, however, the relationship is no longer linear and follows some power law.

B. Temperature dependence

The temperature dependencies of the current-voltage and EL intensity-voltage characteristics are shown in Figs. 5(a) and 5(b), respectively. The current density shows a thermally activated behavior as reported previously.[21] Correspondingly, a large temperature dependence is observed also in the EL intensity. Figure 6 shows the EL intensity as a function of current density at various temperatures. It should be noted that the curves at different temperatures do not overlap each other. This means that the temperature dependence of EL intensity cannot simply be regarded as a result of the change in current density. The critical current density at which the EL intensity becomes proportional to the current density increases with increasing temperature.

C. Excitation-wavelength dependence of the PL quenching

Previously,[20,21] we reported the experimental observation of PL quenching caused by the application of bias voltages in similar solid-state-contact devices. This phenomenon is interpreted as a result of the dissociation of photoexcited excitons by the electric field. Since the penetration depth of the excitation light depends on its wavelength, we can get information on the depth profile of the electric field intensity in the sample by measuring the excitation-wavelength dependence of the PL quenching. In this study we used monochromated light from a 150 W Xe lamp as the excitation source. The experimental result is shown in Fig. 7 by plotting the relative PL intensity at a bias voltage of 50 V versus the excitation wavelength. This result indicates that the quenching is most efficient in the excitation-wavelength range shorter than 380 nm.

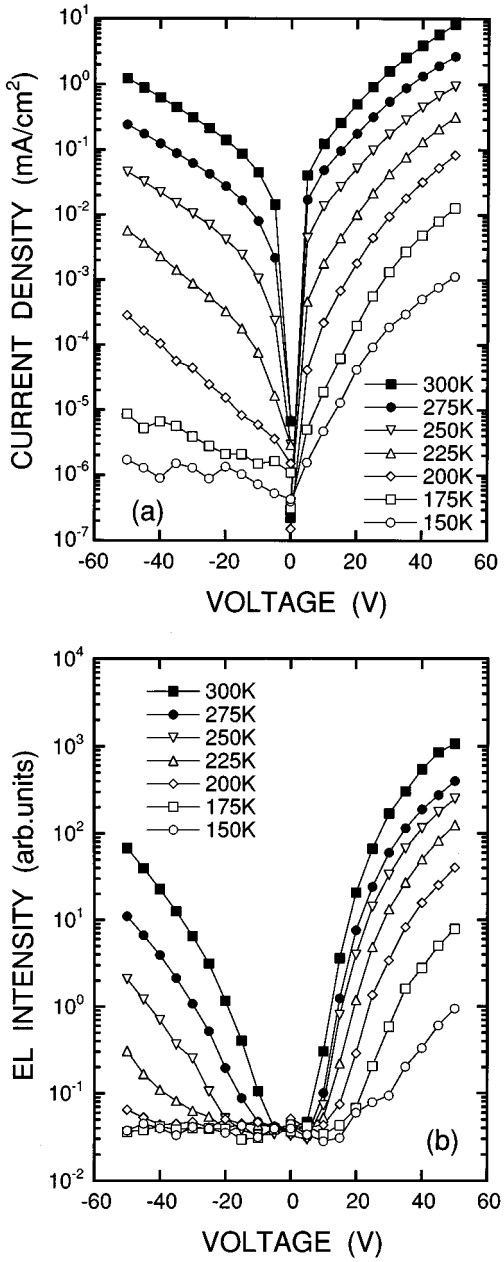

FIG. 5. Current density-voltage curves (a) and EL intensity-voltage curves (b) measured at various temperatures.

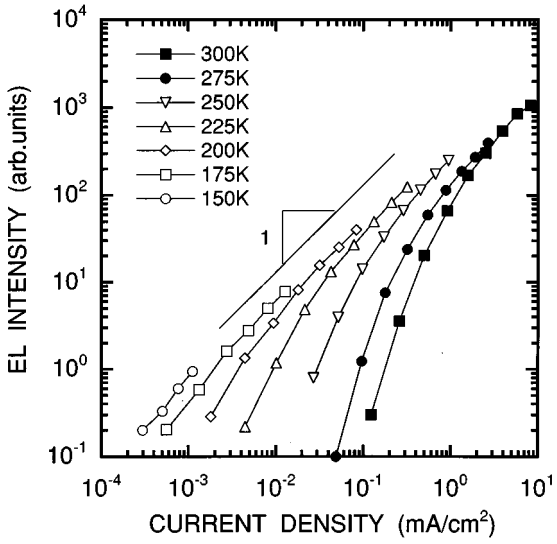

FIG. 6. EL intensity vs current density at various temperatures. The straight line indicates the slope of linear functions.

IV. DISCUSSION

A. Spectral similarity between PL and EL

The similarity in luminescence spectra between PL and EL (Fig. 2) indicates that the same carrier-recombination mechanism is involved in the two phenomena. Therefore, the excitons localized within Si nanocrystallites in PS are likely to be responsible also for the EL.[25–28] The broad and Gaussian shape of the spectrum is due to a large lattice relaxation caused by the strong localization of either of the carriers. As mentioned above, the EL spectrum more closely resembles the PL spectrum obtained from excitation by the shorter-wavelength (325 nm) light, which penetrates only slightly in PS.[29] Thus it is supposed that only the near-surface region in the porous layer emits EL. This is supported further by the existence of a strong electric field near the surface as discussed below. A careful inspection of Fig. 2 reveals that the EL spectrum can be reproduced by cutting off some long-wavelength components from the PL spectrum excited at 325 nm. The lack of the long-wavelength components in the EL spectrum can be explained by the field-induced dissociation of localized excitons, which is expected to be more probable for longer-wavelength components because of their longer excited-state lifetimes. This is similar to what happens to the PL under sufficient electric fields. We have observed in a separate study that the field-induced PL quenching occurs preferentially for the longest-wavelength component as the field strength is increased.[30]

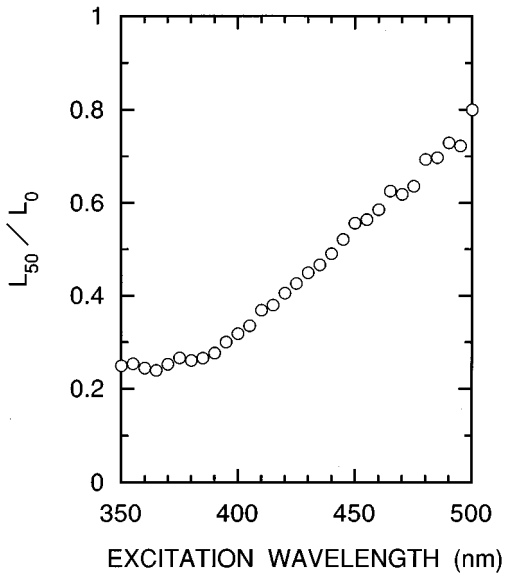

FIG. 7. The PL intensity at an applied bias voltage of 50 V (L_{50}) divided by that without bias (L_0) plotted as a function of excitation wavelength.

B. Relation between EL intensity and current density

A linear relationship is clearly observed between the EL intensity and current density in the regions of sufficient current densities (Figs. 4 and 6). This denies the direct excitation of luminescence centers by accelerated carriers as the principal excitation mechanism of the EL. The localized electron-hole pairs responsible for the visible luminescence, therefore, are supposed to be created by trapping an electron and a hole from the conduction and the valence band, respectively. The observed temperature dependence of EL efficiency in the linear region (Fig. 6) indicates the significance of nonradiative recombination of the trapped carriers. In fact, similar temperature dependence was found also in the PL efficiency of the same sample.

The deviation from the linear relationship at low current densities (Fig. 6) implies that there exists some current component which does not directly contribute to EL. In other words, a significant amount of current precedes the onset of EL. The extrapolated current values at zero EL intensity depend largely on temperature, suggesting this current component to be thermally activated as well as the major diode current.

C. Carrier generation mechanisms

The observed excitation-wavelength dependence of PL quenching (Fig. 7) reflects the distribution of electric field intensity along the depth direction in the sample, since the penetration depth of light depends on its wavelength. Our result indicates that a strong electric field, which is intense enough to cause the maximum PL quenching, exists in the range of a depth roughly corresponding to the penetration depth of light at 380 nm. According to our previous result of photoreflectance spectroscopy for light-emitting PS,[29] the penetration depth at this wavelength may be of the order of several hundred nanometers. If we assume that the major potential drop is produced within this thin near-surface region, the average electric field intensity in that region reaches $\sim 10^6$ V/cm for a bias of several tens of volts. This value is comparable with those required to cause electrical breakdown phenomena in Si *pn* junctions.[31] Because of possible structural inhomogeneity, the local electric field may become more intense.

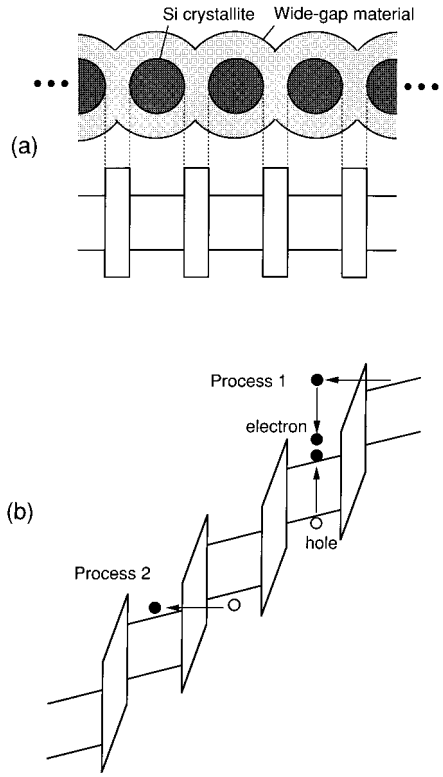

FIG. 8. (a) Upper: illustration of Si nanocrystallites connected via wide-gap regions, which models the nanoscopic structure of light-emitting PS. Lower: corresponding band diagram at thermal equilibrium. (b) Band structure of the Si nanostructure system under a strong electric field. Two possible high-field effects are illustrated; process 1 (electron-hole-pair generation by energetic hot electrons) and process 2 (tunneling injection of electrons from the valence band).

Each nanocrystallite in light-emitting PS is supposed to be surrounded by a wide bandgap region since it behaves like a quantum dot.[32] The wide gap region may be composed of oxides, hydrides, amorphous Si, or simply a Si nanostructure of smaller dimensions. Thus, the microscopic structure of PS along the direction of current flow can be illustrated like Fig. 8(a), where Si nanocrystallites are connected together via wider-gap interface regions. When a bias voltage is applied to this ensemble, a stronger electric field may build up preferentially in the wide-gap regions because of their expected lower dielectric constant and higher resistivity. Then, the conduction and valence band edges of the nanocrystallites become shifted with respect to those of respective neighboring ones. This band shift increases with increasing the applied voltage. Under a sufficiently large bias voltage, therefore, a critical situation would appear locally: the energy position of the valence-band edge of a crystallite becomes comparable with that of the conduction-band edge of the neighboring one, as shown in Fig. 8(b).

In this situation, either of the following two phenomena are expected to occur. First, hot electrons injected from the conduction band of a crystallite into the conduction band of the neighboring one are so energetic that they can create electron-hole pairs by an impact process (process 1). Second, electron-hole pairs can be created also by the tunneling of electrons from the valence band of a crystallite into the conduction band of the next one (process 2). Progress of these processes should significantly increase the number of carriers in the PS layer, and consequently led to a sharp increase in current density at the corresponding voltage. This is similar to the electrical breakdown in reverse biased *pn* junctions. Although at this stage we can not speculate which process is predominant in our devices, the reported high quantum efficiency in photocurrent[33] could reflect an avalanche-like effect due to cascade of process 1. In any case, it is important to note that holes are generated by these processes, which makes the radiative recombination possible even in the structure with no *pn* junctions.

D. Device operation model

Based on the above discussions, we propose the following model for the operation of the metal/PS/*n*-Si EL device. Because of a significantly high resistivity of the PS layer, only a little amount of current can flow under low bias voltages. This current should be mainly due to the flow of electrons. This is because the current in this low voltage range is not directly linked with EL, as indicated by Fig. 6, and therefore virtually only one type of carrier should be involved. These electrons may originate from the substrate or the metal contact, depending on the polarity of bias.

When the bias voltage is increased to a certain value, a significant amount of current begins to flow as a result of either of the carrier generation mechanisms mentioned above. If we use the usual exponential relationship to describe the current-voltage behavior of this device, therefore, the suddenly increasing character of current at a relatively high voltage may be expressed by an extremely large value of the diode ideality factor. The experimentally obtained value of greater than one hundred can easily be explained by this mechanism.

Part of the generated carriers can then recombine radiatively via localized states as mentioned above. However, since the mean electric-field strength is very high near the regions where the field-induced carrier generation occurs, most of the generated electrons and holes are immediately separated and swept away toward opposite directions. Thus the overlap of the electron and hole population is limited within a very thin layer close to the surface metal contact. Therefore, the radiative recombination of carriers is possible only near the surface of PS. This is why the EL spectrum is close to the PL spectrum for the shorter-wavelength excitation as shown in Fig. 2. The spectral similarity in EL between forward and reverse bias[22] implies that the high-electric-field region is produced near the PS surface independent of polarity. This is consistent with the poor rectifying properties shown in Figs. 3 and 5(a).

The small overlap between electron and hole populations results in the relatively low EL efficiency. In other words, the strong electric field which causes EL by creating carriers also limits the EL efficiency because of the separation of the carriers. In order to reduce this undesirable effect, it is necessary to create holes without the help of a strong electric field. Efficient devices, therefore, should be implemented on the basis of a low-electric-field carrier-injection mechanism by, for example, sandwiching the PS layer between *p*- and

n-type materials with a larger band-gap energy (i.e., by introducing the double-heterojunction structure). Elimination of the high-electric-field region from the device configuration may also provide favorable effects on the stability of the device operation. Although some attempts to introduce a single heterojunction into the device structure have been pursued, no significant improvements have been attained in EL efficiency and operating bias voltage.[12,34] This implies that low-bias carrier injection from bulk Si into PS layers is difficult, which may be due to an increased band gap of the Si nanocrystallites in PS.

V. CONCLUSION

An operation model for the metal/PS/*n*-Si EL device has been proposed based on some experimental results on its fundamental characteristics. In our model, holes as well as the majority of electrons are created in the PS layer by either of the following two possible field-induced processes; impact excitation by energetic hot electrons and tunneling of valence-band electrons into the conduction band of neighboring crystallites. A fraction of the generated carriers then contribute to EL by radiative recombination via localized states in Si nanocrystallites. There is, however, a limitation in the EL efficiency, since most of the generated carriers are immediately separated by the strong electric field. Establishment of a low-bias carrier-injection scheme is necessary to obtain a substantial improvement in the EL characteristics. Introduction of the double heterostructure made by sandwiching the PS layer between *p*- and *n*-type wide-gap materials is promising.

ACKNOWLEDGMENTS

This work is supported in part by the Research Foundation for Opto-Science and Technology, Nissan Science Foundation, and a Grant-in-Aid for Scientific Research from the Ministry of Education, Science, Sports and Culture of Japan.

[1] S. S. Iyer and Y.-H. Xie, Science **260**, 40 (1993).
[2] L. Brus, J. Phys. Chem. **98**, 3575 (1994).
[3] D. J. Lockwood, Solid State Commun. **92**, 101 (1994).
[4] B. Hamilton, Semicond. Sci. Technol. **10**, 1187 (1995).
[5] L. T. Canham, Appl. Phys. Lett. **57**, 1046 (1990).
[6] A. Bsiesy, J. C. Vial, F. Gaspard, R. Herino, M. Ligeon, F. Muller, R. Romestain, A. Wasiela, A. Halimaoui, and G. Bomchil, Surf. Sci. **254**, 195 (1991).
[7] N. Koshida and H. Koyama, Jpn. J. Appl. Phys. **30**, L1221 (1991).
[8] A. Halimaoui, C. Oules, G. Bomchil, A. Bsiesy, F. Gaspard, R. Herino, M. Ligeon, and F. Muller, Appl. Phys. Lett. **59**, 304 (1991).
[9] L. T. Canham, W. Y. Leong, M. I. J. Beale, T. I. Cox, and L. Taylor, Appl. Phys. Lett. **61**, 2563 (1992).
[10] N. Koshida and H. Koyama, Appl. Phys. Lett. **60**, 347 (1992).
[11] A. Richter, P. Steiner, F. Kozlowski, and W. Lang, IEEE Electron Device Lett. **12**, 691 (1991).
[12] F. Namavar, H. P. Maruska, and N. M. Kalkhoran, Appl. Phys. Lett. **60**, 2514 (1992).
[13] P. Steiner, F. Kozlowski, and W. Lang, Appl. Phys. Lett. **62**, 2700 (1993).
[14] A. Loni, A. J. Simons, T. I. Cox, P. D. J. Calcott, and L. T. Canham, Electron. Lett. **31**, 1288 (1995).
[15] C. Peng and P. M. Fauchet, Appl. Phys. Lett. **67**, 2515 (1995).
[16] P. Steiner, F. Kozlowski, M. Wielunski, and W. Lang, Jpn. J. Appl. Phys. **33**, 6075 (1994).
[17] N. Koshida, H. Koyama, Y. Yamamoto, and G. J. Collins, Appl. Phys. Lett. **63**, 2655 (1993).
[18] K. Li, D. C. Diaz, Y. He, J. C. Campbell, and C. Tsai, Appl. Phys. Lett. **64**, 2394 (1994).
[19] J. Wang, F.-L. Zhang, W.-C. Wang, J.-B. Zheng, X.-Y. Hou, and X. Wang, J. Appl. Phys. **75**, 1070 (1994).
[20] H. Koyama, T. Oguro, and N. Koshida, Appl. Phys. Lett. **62**, 3177 (1993).
[21] T. Ozaki, T. Oguro, H. Koyama, and N. Koshida, Jpn. J. Appl. Phys. **34**, 946 (1995).
[22] F. Kozlowski, M. Sauter, P. Steiner, A. Richter, H. Sandmaier, and W. Lang, Thin Solid Films **222**, 196 (1992).
[23] L. Pavesi, M. Ceschini, G. Mariotto, E. Zanghellini, O. Bisi, M. Anderle, L. Calliari, M. Fedrizzi, and L. Fedrizzi, J. Appl. Phys. **75**, 1118 (1994).
[24] Z. Chen, T.-Y. Lee, and G. Bosman, J. Appl. Phys. **76**, 2499 (1994).
[25] H. Koyama, N. Shima, T. Ozaki, and N. Koshida, Jpn. J. Appl. Phys. **33**, L1737 (1994).
[26] H. Koyama and N. Koshida, Phys. Rev. B **52**, 2649 (1995).
[27] H. Koyama, T. Ozaki, and N. Koshida, Phys. Rev. B **52**, R11 561 (1995).
[28] H. Koyama, N. Shima, and N. Koshida, Phys. Rev. B **53**, R13 291 (1995).
[29] N. Koshida, H. Koyama, Y. Suda, Y. Yamamoto, M. Araki, T. Saito, K. Sato, N. Sata, and S. Shin, Appl. Phys. Lett. **63**, 277 (1993).
[30] T.Ozaki, T. Oguro, H. Koyama, and N. Koshida (unpublished).
[31] S. M. Sze, *Physics of Semiconductor Devices*, 2nd ed. (Wiley, New York, 1981), Chap. 2.
[32] S. Schuppler, S. L. Friedman, M. A. Marcus, D. L. Adler, Y.-H. Xie, F. M. Ross, T. D. Harris, W. L. Brown, Y. J. Chabal, L. E. Brus, and P. H. Citrin, Phys. Rev. Lett. **72**, 2648 (1994).
[33] J. P. Zheng, K. L. Jiao, W. P. Shen, W. A. Anderson, and H. S. Kwok, Appl. Phys. Lett. **61**, 459 (1992).
[34] T. Futagi, T. Matsumoto, M. Katsuno, Y. Ohta, H. Mimura, and K. Kitamura, Jpn. J. Appl. Phys. **31**, L616 (1992).